Side-Chain Rotational Isomerization in Proteins: A Mechanism Involving Gating and Transient Packing Defects

J. A. McCammon,*† C. Y. Lee,§ and S. H. Northrup‡

Contribution from the Departments of Chemistry, University of Houston, Houston, Texas 77004, and Tennessee Technological University, Cookeville, Tennessee 38501.
Received September 15, 1982

Abstract: Tyrosine ring rotational isomerization trajectories from a dynamical simulation are analyzed to clarify the involvement of structural fluctuations in the surrounding protein matrix. The correlation of matrix atom displacements with ring rotation is determined by examination of both ensemble averages and time sequences of protein configurations. Transient packing defects are quantitatively assessed by the Voronoi polyhedron method. The results show that the isomerization is a gated process, in which the ring rotation is systematically preceded by the spontaneous displacement of a section of adjacent backbone. This displacement creates a transient packing defect (~ 10 Å^3) that helps to initiate the transition and reduces the energy barrier for the transition proper by relieving unfavorable van der Waals contacts. The results are discussed in the context of current models for motion in proteins, liquids, and solids.

Globular proteins have well-defined, densely packed structures in the native state.[1] Despite this, the forces that maintain their three-dimensional structures are sufficiently weak that native proteins exhibit substantial atomic mobility at ordinary temperatures.[2-5] Proteins are therefore somewhat permeable to small molecules[6,7] and display considerable conformational lability on a local scale.[8] These features, which are essential to much of protein function,[2-5] raise important mechanistic questions. Given the severe steric constraints imposed by the dense packing, how does a small molecule move from one location to another in a protein? How does a bulky group such as a side chain that is encaged by neighboring groups in the protein change its conformation?

An attractive model that has been proposed for such local structure changes pictures these changes as arising from transient packing defects in the protein interior.[9-12] In a limiting version of the model, it could be assumed that the displacement of a group depends on the spontaneous formation of a cavity that is sufficiently large for the group to jump into. This is analogous to the simple free volume model of diffusion in liquids.[13] Richards has considered the energetics of such local volume fluctuations in proteins.[11] He showed that the free volume model could reasonably account for small molecule diffusion in those regions of proteins where native packing defects exist; the expansion of such defects to the required size involves typical thermal energies. More generally, group displacements in proteins could be imagined to result from the formation of a succession of smaller packing defects in the protein. Computer simulations of atomic motion in simple liquids indicate that this is a more accurate model for these systems; the atoms are driven into small, transient vacancies by collisions from the side opposite the vacancy.[14]

A complementary model for large atomic displacements in proteins pictures the motion as resulting from transient relaxation of steric barriers that separate more stable atomic configurations. Here, it is assumed that certain "gate" atoms of the protein matrix spontaneously part, allowing the displaced group to jump past to a new position. This is analogous to the vacancy mechanism for diffusion in solids.[15] Experimental[16] and theoretical[17] studies of ligand motion in oxygen-binding heme proteins are consistent with this type of mechanism.

Quite recently, a dynamical simulation method has been developed that allows the detailed analysis of large displacements of groups in proteins.[18-20] The simulation method consists of two parts. In the first, one calculates the free energy barrier for the process of interest.[20] In the present connection, this barrier separates two comparatively stable local conformations and is dominated by van der Waals repulsion between the displaced group and its neighbors. The second step consists of the calculation of a representative set of trajectories for the process using information on the location of the energy barrier.[18-20] This method has been applied to study the rotational isomerization of a tyrosine ring in the interior of a small protein, the bovine pancreatic trypsin inhibitor (BPTI).[18-20] It was found that collisions between the ring and atoms in the surrounding protein matrix govern the ring rotational dynamics. A significant fraction of the transition attempts are unsuccessful due to collisions in the transition-state region that knock the ring back toward its initial state. The transition attempts themselves result from transient decreases in the frequency of collisions that would tend to drive the ring away from the barrier; this suggests that transient packing defects play a role in initiating the rotations.[19]

In this paper, we analyze the structural changes in the protein matrix that are involved in the rotational isomerization of the tyrosine ring. Computer-simulated trajectories of both successful and unsuccessful transition attempts are considered. Changes in

† University of Houston.
§ Department of Chemistry, Iowa State University, Ames, IA 50011.
‡ Tennessee Technological University.

(1) Richards, F. M. *Annu. Rev. Biophys. Bioeng.* **1977**, *6*, 151.
(2) McCammon, J. A.; Karplus, M. *Acc. Chem. Res.*, in press.
(3) Karplus, M.; McCammon, J. A. *Annu. Rev. Biochem.*, in press.
(4) Debrunner, P. G.; Frauenfelder, H. *Annu. Rev. Phys. Chem.* **1982**, *33*, 283.
(5) Jardetzky, O. *Acc. Chem. Res.* **1981**, *14*, 291.
(6) Woodward, C. K.; Hilton, B. D. *Annu. Rev. Biophys. Bioeng.* **1979**, *8*, 99.
(7) Weber, G. *Adv. Protein Chem.* **1975**, *29*, 1.
(8) Campbell, I. D.; Dobson, C. M.; Williams, R. J. P. *Adv. Chem. Phys.* **1978**, *39*, 55.
(9) Lumry, R.; Rosenberg, A. *Collect. Int. C.N.R.S. L'eau. Syst. Biol.* **1975**, *246*, 55.
(10) Cooper, A. *Proc. Natl. Acad. Sci. U.S.A.* **1976**, *73*, 2740.
(11) Richards, F. M. *Carlsberg Res. Commun.* **1979**, *44*, 47.
(12) Wagner, G. *FEBS Lett.* **1980**, *112*, 280.
(13) Egelstaff; P. A. "An Introduction to the Liquid State"; Academic Press: New York, 1967; Chapter 10.
(14) Rahman, A. *J. Chem. Phys.* **1966**, *45*, 2585.
(15) Bennett, C. H. In "Diffusion in Solids"; Burton, J. J., Nowick, A. S., Eds.; Academic Press: San Francisco, CA, 1975; pp 73-113.
(16) Austin, R. H.; Beeson, K. W.; Eisenstein, L.; Frauenfelder, H.; Gunsalus, I. C. *Biochemistry* **1975**, *14*, 5355.
(17) Case, D. A.; Karplus, M. *J. Mol. Biol.* **1979**, *132*, 343.
(18) McCammon, J. A.; Karplus, M. *Proc. Natl. Acad. Sci. U.S.A.* **1979**, *76*, 3585.
(19) McCammon, J. A.; Karplus, M. *Biopolymers* **1980**, *19*, 1375.
(20) Northrup, S. H.; Pear, M. R.; Lee, C. Y.; McCammon, J. A.; Karplus, M. *Proc. Natl. Acad. Sci. U.S.A.* **1982**, *79*, 4035.

0002-7863/83/1505-2232$01.50/0

the free volume around the ring are quantitatively monitored by use of the Voronoi polyhedron method; this method has been used successfully in earlier studies of atomic structure and motion in liquids[14,21,22] and atomic packing in static protein structures.[11,23-26] Matrix atoms that have sizable displacements correlated with the ring rotation are identified. These results are used to define a mechanism for the rotational isomerization process. Transient packing defects and gating are both essential components in this mechanism.

Methods

Trajectory Calculations. The calculation of the trajectories that are analyzed here has been described previously.[20] In the first part of the calculation, a modified molecular dynamics algorithm was used to generate sets of protein configurations that are constrained to lie within selected windows of a reaction coordinate ξ for the rotational isomerization. By an appropriate analysis of data from overlapping windows, the free energy of the system as a function of ξ was calculated; this free energy is termed the potential of mean force for the ring rotation. The reaction coordinate is a linear combination of two dihedral angles, $\xi = \chi_{35}^2 - \chi_v$. The angle χ_{35}^2 is the standard ring dihedral angle (C_{35}^{α}–C_{35}^{β}–C_{35}^{γ}–$C_{35}^{\delta 1}$). The angle χ_v is a virtual dihedral angle (C_{35}^{β}–C_{35}^{γ}–$C_{35}^{\delta 2}$–N_{36}) that reflects the orientation of the ring plane relative to the local backbone; inclusion of such a term in ξ is essential because nonbonded contacts between the ring and the backbone make a major systematic contribution to the barrier to isomerization. The form for ξ was originally chosen on empirical grounds; this choice is justified on physical grounds in the present work by examination of an adiabatic χ_{35}^2, χ_v potential surface and isomerization trajectories in the χ_{35}^2, χ_v plane.

In the second part of the calculation, 200 independent trajectories were calculated from initial states in the region of the free energy barrier maximum. Twelve of these were continued forward and backward in time as described previously[18,19] to yield complete trajectories of 3-ps duration for detailed analysis. Six of these trajectories correspond to successful transitions and six to unsuccessful transitions that returned to the original stable ring orientation following collisions in the transition-state region.

That only 12 trajectories have been subjected to detailed analysis may raise questions concerning the statistical significance of the results obtained. In particular, if the trajectories originated from similar configurations, one could expect to observe similarities in the results. To minimize this possibility, the 12 trajectories were developed from configurations that are separated by intervals of approximately 6 ps in the dynamical simulation of the transition-state region. This interval is an order of magnitude longer than the equilibrium correlation time of the ring angular velocity or orientation (both ~0.2 ps) and is sufficient to randomize large-scale features of the protein structure.[2,3] Thus, the 12 trajectories are completely independent.

Adiabatic χ_{35}^2, χ_v Potential Surface. To calculate an adiabatic potential energy surface as a function of χ_{35}^2 and χ_v, the following procedure was used; this procedure is an extension of that used previously to calculate the adiabatic potential as a function of χ_{35}^2 alone.[27,28] The reference BPTI structure is one obtained from a 16-ps dynamical equilibration of the entire protein.[20] Atoms more than 7.7 Å from the tyrosine ring centroid were fixed in this structure, and the remaining 94 atoms were subjected to 500 cycles of steepest descent energy minimization. The ring was then rotated around the C_{35}^{β}–C_{35}^{γ} axis to generate 12 conformations defined by $\chi_{35,i}^2 = 20°, 40°, ..., 240°$; for each conformation i, the resulting value of χ_v was calculated and denoted by $\chi_{v,i}$. Starting with each of these 12 conformations, nine energy minimization calculations were carried out. The calculation j starting from conformation i was subject to the constraint potentials

$$U_2(\chi_{35}^2) = k_2 (\chi_{35}^2 - \chi_{35,i}^2 + 10j/\pi)^2$$

$$j = 0, \pm 1, ..., \pm 4$$

$$U_v(\chi_v) = k_v(\chi_v - \chi_{v,i})^2$$

where k_2 = 300 kcal mol^{-1} rad^{-2} and k_v = 50 kcal mol^{-1} rad^{-2}. Each energy minimization consisted of 200 steepest descent cycles. The surface was constructed from the relaxed values of χ_{35}^2, χ_v and potential energy resulting from each of the 108 separate minimizations.

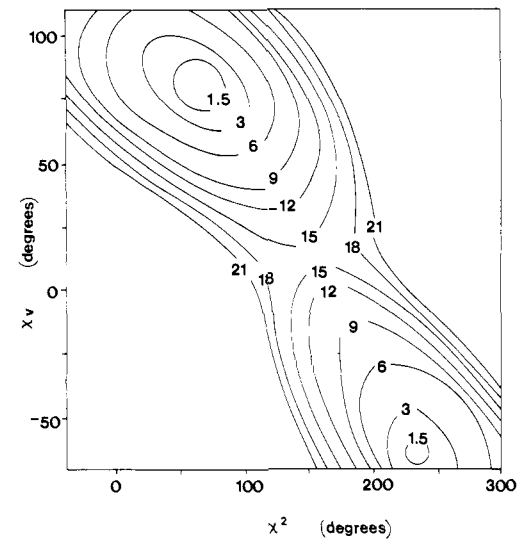

Figure 1. Adiabatic potential surface for rotational isomerization of the tyrosine ring. The contours are in units of kilocalories per mole.

Voronoi Polyhedron Volumes. The conventional Voronoi polyhedron associated with an atom is the volume bounded by planes that are perpendicular to and bisect the lines that connect the atom to all neighboring atoms. Efficient programs for calculating such polyhedra exist, and one of these was used in the present work.[29] In the analysis of the tyrosine ring rotations, it was necessary to calculate for several ring atoms that portion of the Voronoi volume that lies on either side of the ring plane. The volume on one side of the ring plane was easily calculated by locating a dummy atom on the other side of plane and very close to the atom of interest.

Time-Independent Results

Adiabatic Potential Surface. The adiabatic potential energy surface as a function of χ_{35}^2 and χ_v for the dynamically equilibrated protein is shown in Figure 1. The two minima corresponding to the stable orientations of the ring are located near $\chi_{35}^2 = 65°$, $\chi_v = 80°$ and $\chi_{35}^2 = 235°$, $\chi_v = -65°$; the corresponding values of ξ are −15° and 300°, respectively. The high-energy regions arise predominantly from local stresses. For example, displacements in the direction of increasing χ_{35}^2 from the $\xi = -15°$ minimum lead to close contacts between O_{35} or C_{35} and $C_{35}^{\delta 2}$, while corresponding displacements in the direction of decreasing χ_v lead to substantial bond angle deformations in the backbone of residue 35 and close contacts between N_{36} and C_{35}^{β}. There is a saddle point on the surface near $\chi_{35}^2 = 155°$, $\chi_v = 15°$ ($\xi = 140°$); important contributions to the energy in this region come from close contacts between N_{36} or C_{35} and $C_{35}^{\delta 2}$. It is clear from Figure 1 that the preferred reaction path is nearly a straight line through the minima and the saddle point. This path is nearly perpendicular to lines of constant ξ on the χ_{35}^2, χ_v plane, which is why ξ is a good reaction

(21) Bernal, J. D. *Nature (London)* **1960**, *185*, 68.
(22) David, E. E.; David, C. W. *J. Chem. Phys.* **1982**, *76*, 4611.
(23) Richards, F. M. *J. Mol. Biol.* **1974**, *82*, 1.
(24) Finney, J. L. *J. Mol. Biol.* **1975**, *96*, 721.
(25) Finney, J. L. *J. Mol. Biol.* **1978**, *119*, 415.
(26) Chothia, C. *Nature (London)* **1975**, *254*, 304.
(27) Gelin, B. R.; Karplus, M. *Proc. Natl. Acad. Sci. U.S.A.* **1975**, *72*, 2002.
(28) Hetzel, R.; Wüthrich, K.; Deisenhofer, J.; Huber, R. *Biophys. Struct. Mech.* **1976**, *2*, 159.
(29) Brostow, W.; Dussault, J. P.; Fox, B. *J. Comput. Phys.* **1978**, *29*, 81.

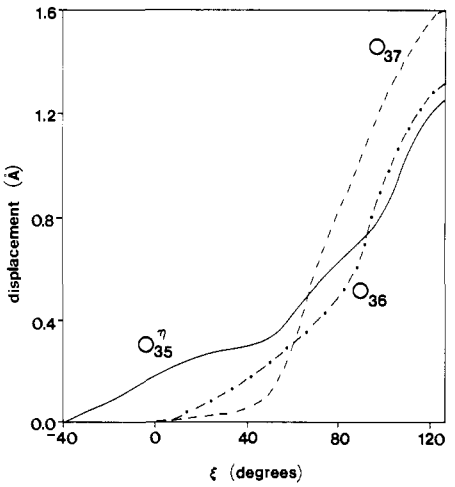

Figure 2. Ensemble-average displacements of selected atoms as obtained from configurations generated during the potential of mean force calculation.

coordinate for the ring rotational isomerization.

The adiabatic potential along the line joining the two stable states provides an approximation to the potential of mean force $W(\xi)$ for the rotational isomerization. An improved approximation that includes thermal effects has been calculated by a constrained molecular dynamics procedure.[20] The improved potential is similar to the adiabatic one, but the minimum corresponding to the X-ray structure occurs at $\xi = -30°$ and the barrier peak occurs at $\xi = 125°$.

Local Structural Changes along the Reaction Coordinate. The above results, and those of previous static[27,28] and dynamic[18-20] studies of ring rotation, demonstrate that important contributions to the effective energy barrier arise from contacts between ring atoms and atoms of the amide linkage between residues 35 and 36. Other local atoms that might provide steric hindrance to the ring rotation are separated from the ring by more than three or four covalent bonds and hence can move away from the ring somewhat more readily. The corresponding nonbonded contributions to the barrier are markedly reduced by relaxation in the static studies and, on the average, by structural fluctuations in dynamic studies.

To obtain a better understanding of the nature of the atomic fluctuations that reduce the effective barrier to ring rotation, we examined the various protein configurations that were generated in the original potential of mean force calculation. Apart from the δ- and ϵ-carbons of the ring, only a few atoms were found to exhibit systematic ensemble-average displacements exceeding 0.5 Å as the ring moved from the minimum in the potential of mean force near $\xi = -30°$ to the transition-state region near $\xi = 125°$. These atoms are C^{ζ}_{35}, O^{η}_{35}, and the backbone group O_{36}, N_{37}, C^{α}_{37}, C_{37}, and O_{37}. The average displacements of several of these atoms as functions of ξ are shown in Figure 2. The sizable displacements of C^{ζ}_{35} and O^{η}_{35} suggest that an important reorientation of the ring rotational axis (through C^{γ} and C^{ζ}) occurs during rotational isomerization. The sizable displacement of the O_{36}–O_{37} group suggests that this backbone segment, which lies above one face of the ring in the stable state, must move substantially to allow room for the ring to rotate. These suggestions are verified by an examination of the time-dependent correlations of the motions, as described below.

Time-Dependent Results

In this section, we present detailed results for one of the successful trajectories that has been subjected to extensive analysis. We also compare these results with those obtained for the other successful and unsuccessful trajectories that have been similarly analyzed.

Time Evolution of Rotational Coordinates. In Figure 3a we show the conventional representation[18,19] of the ring rotation, in which the rotation angle Φ of the ring plane around the axis through

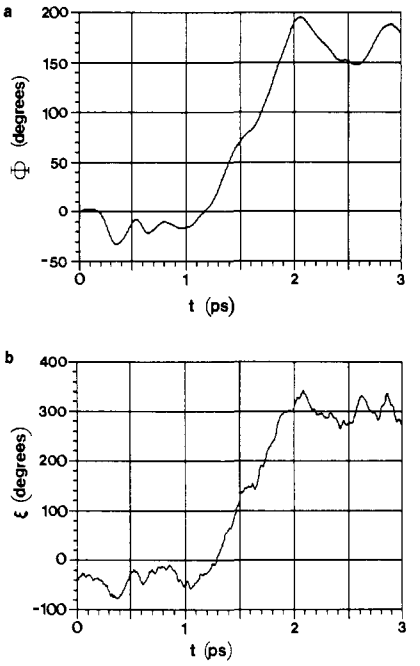

Figure 3. Rotation of the tyrosine ring plane about the C^{γ}_{35} – C^{ζ}_{35} axis (a) and variation of the reaction coordinate ξ (b) during the rotational isomerization.

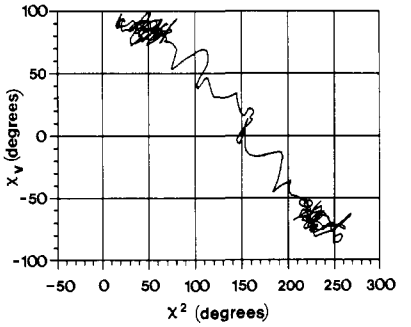

Figure 4. Evolution of the dihedral angles χ^2_{35} and χ_v during the rotational isomerization.

C^{γ}_{35} and C^{ζ}_{35} is displayed as a function of time. A corresponding plot of $\xi(t)$ is given in Figure 3b. The rotation is of the ideal transition state type,[18-20] in which only a slight slowing of the rotation occurs as the ring approaches the barrier maximum. Four of the successful trajectories exhibit this type of behavior. Of the other two, one exhibits substantial damping after crossing the transition-state region (the magnitude of the slope between 1.5 and 2.0 ps is roughly half that between 1.0 and 1.5 ps), and the other exhibits a near reversal in the transition-state region (the slope falls to zero at 1.4 ps). These properties, and the 1-ps times required to complete the transitions, are consistent with previous results.[18-20] Of the six unsuccessful trajectories, three are immediately reflected from the transition-state region toward the initial state region and three remain in the transition-state region for about 0.5 ps before returning to the initial state. No cases were observed in which the trajectory moved beyond $\xi = 140°$ and subsequently returned to the initial state.

In Figure 4, we show the evolution of the ring rotation trajectory in the χ_v, χ^2_{35} plane. The progress of the motion along the reaction coordinate ξ during the transition is apparent, as are vibrations of smaller amplitude in the direction perpendicular to the reaction coordinate. Overall, the motion is consistent with the general features of the adiabatic potential surface shown in Figure 1. Similar characteristics are evident for the other successful trajectories, although those that pass more slowly through the transition region tend to show correspondingly more tortuous motion in that region. An interesting feature of most of the unsuccessful trajectories is a displacement in the χ_v direction

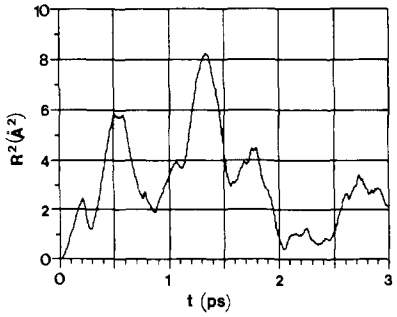

Figure 5. Sum of the squared displacements of O_{36}, N_{37}, C^{α}_{37}, C_{37}, and O_{37} during the rotational isomerization.

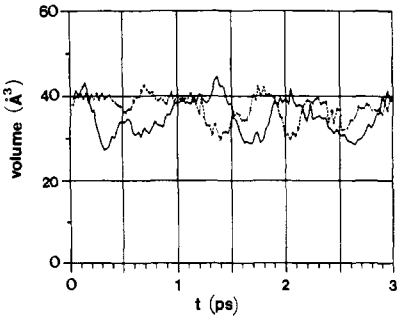

Figure 6. Sum of the partial Voronoi polyhedra volumes V_+ (—) and V_- (---) during the rotational isomerization. The volumes V_+ and V_- are defined in the text.

during the period of trajectory reversal in the transition-state region; this suggests that the transition attempts are aborted by fluctuations in the local backbone that result in unfavorable collisions with the ring.

Local Structural Changes during the Ring Rotation. In Figure 5, we show the sum of the squared displacements R^2 of the five backbone atoms O_{36}, N_{37}, C^{α}_{37}, C_{37}, and O_{37} as a function of time. The displacements are relative to the positions of the atoms at $t = 0$. The sum reaches a maximum of 8 Å^2 at 1.3 ps, corresponding to the time at which the ring rotational transition begins (cf. Figure 3). The maximum value of this sum is substantially larger than that expected for a typical fluctuation; for atoms with independent mean-square fluctuations of 1 Å^2, a typical maximum in the sum would be on the order of $(5)^{1/2}$ (1 Å^2) = 2.2 Å^2. Similar results were obtained for most of the other successful and unsuccessful trajectories.

These results support the conclusion drawn from the time-independent analysis that the displacement of this backbone group plays an important role in the rotational isomerization process. That the backbone displacement systematically precedes the transition suggests that the isomerization is a "gated" reaction; that is, the rate of the isomerization is limited by the frequency of occurrence of transient local configurations within which the barrier to ring rotation is relatively low. Of the five backbone atoms that appear to comprise a key element in the gate, only O_{37} has a significant solvent exposure according to a Richards analysis of the X-ray structure.[1]

The reorientation of the rotational axis during isomerization that was suggested by time-independent analysis is also observed in most of the successful and unsuccessful trajectories. In a typical case, the displacement of O^{η} from its $t = 0$ position attains a value between 2 and 4 Å as the ring moves through the transition-state region.

Local Volume Changes during the Ring Rotation. In Figure 6, we show the time dependence of two sums of Voronoi polyhedra volumes for the δ- and ϵ-carbons of the ring. The solid curve corresponds to the volume V_+ into which these atoms tend to move upon an increase in Φ (i.e., those portions of the $C^{\delta 1}$ and $C^{\epsilon 1}$ polyhedra that lie below the plane of the ring plus those portions of the $C^{\delta 2}$ and $C^{\epsilon 2}$ polyhedra that lie above the plane of the ring, when the ring is viewed along the direction from C^{ζ} to C^{γ} with $C^{\delta 2}$ on the viewer's right-hand side). The dotted curve corresponds to the volume V_- into which the δ- and ϵ-carbons of the ring tend to move upon a decrease in Φ. It is apparent that there is a transient increase of V_+ by about 10 Å^3 preceding the transition and that this volume decreases during the transition. The opposite behavior is observed in V_-. Similar characteristics are evident in most of the other successful trajectories. It is of interest that in the successful trajectory that exhibits substantial damping after crossing the transition-state region, there is no apparent drop in V_+ or rise in V_- after $t = 1.5$ ps. Among the unsuccessful trajectories, there is a distinct tendency for V_+ to exceed V_- both before and after the approach to the transition-state region.

These results confirm the tentative conclusion drawn from an earlier analysis of the collisions between ring and matrix atoms that small, transient packing defects facilitate and initiation of isomerization.[19] It is also clear that the transitions do not occur by a simple free volume mechanism; there is no tendency for a large vacancy to appear within which the ring can freely rotate.[12,30]

Visualization of the Ring Rotation. In Figure 7, we show a sequence of actual configurations from the rotational isomerization trajectory represented in Figures 3 through 6. Many of the previously described features of the transition are clearly apparent, as are relationships among some of these features. In the first structure shown ($t = 0.5$ ps), the ring is seen to be sandwiched between the backbone of residue 37 on the top and the side chains of residues 33 and 44 on the bottom. During the period from 0.75 to 1.25 ps, before the ring begins to rotate appreciably, the backbone of residue 37 moves upward. This displacement allows the ring to swing upward away from residues 33 and 44; there is a concomitant reorientation of the axis through C^{γ}_{35} and C^{ζ}_{35} and increase in the volume V_+. Subsequently, the ring rotates, resulting in a close approach of $C^{\delta 2}_{35}$ and N_{36} that is apparent at 1.5 ps. Between 1.38 and 2.0 ps, the backbone of residue 37 returns to a configuration similar to its initial one.

Discussion

The results described here represent a significant addition to our understanding of large atomic displacements in proteins. They make clear how a localized process such as the rotational isomerization of a side chain can be essentially coupled to collective motions in the surrounding protein matrix. In the present case, it is clear that the rotation of a tyrosine ring in BPTI is systematically preceded by the spontaneous displacement of a section of adjacent backbone. This displacement has two effects. First, it helps to initiate the transition by creating a small cavity toward which the ring is driven by collisions with the remaining nearby matrix atoms. Second, it reduces the energy barrier for the transition proper by providing partial relief from highly unfavorable van der Waals contacts that would occur in the locally collapsed matrix. These two aspects of the rotational isomerization mechanism are respectively termed transient packing defect and gating effects. It seems likely that these effects would play a role in the group motions involved in ligand binding, enzyme action, and other biological processes.

There are several issues that have been raised here that warrant further study. It will be desirable to decompose the energetic and kinetic contributions of gating per se and the intrinsic displacement of a group through the matrix in the gate-open configuration. Previous calculations for the ring rotational isomerization show that the ring-matrix nonbonded repulsions amount only to a few kilocalories per mole in typical transition-state configurations.[19] Thus, much of the free energy of activation appears to arise from the deformation of the surrounding matrix into its gate-open configuration. If this is the case, frictional and other effects associated with the gate atoms as well as those associated with the ring itself may influence the transition kinetics. This would be reflected in experimental parameters such as the activation volume of the transition.[12,30] In processes where the gate motions involve displacements at the protein surface, local processes that appear to be intrinsically confined to the protein interior may

(30) Karplus, M.; McCammon, J. A. *FEBS Lett.* **1981**, *131*, 34.

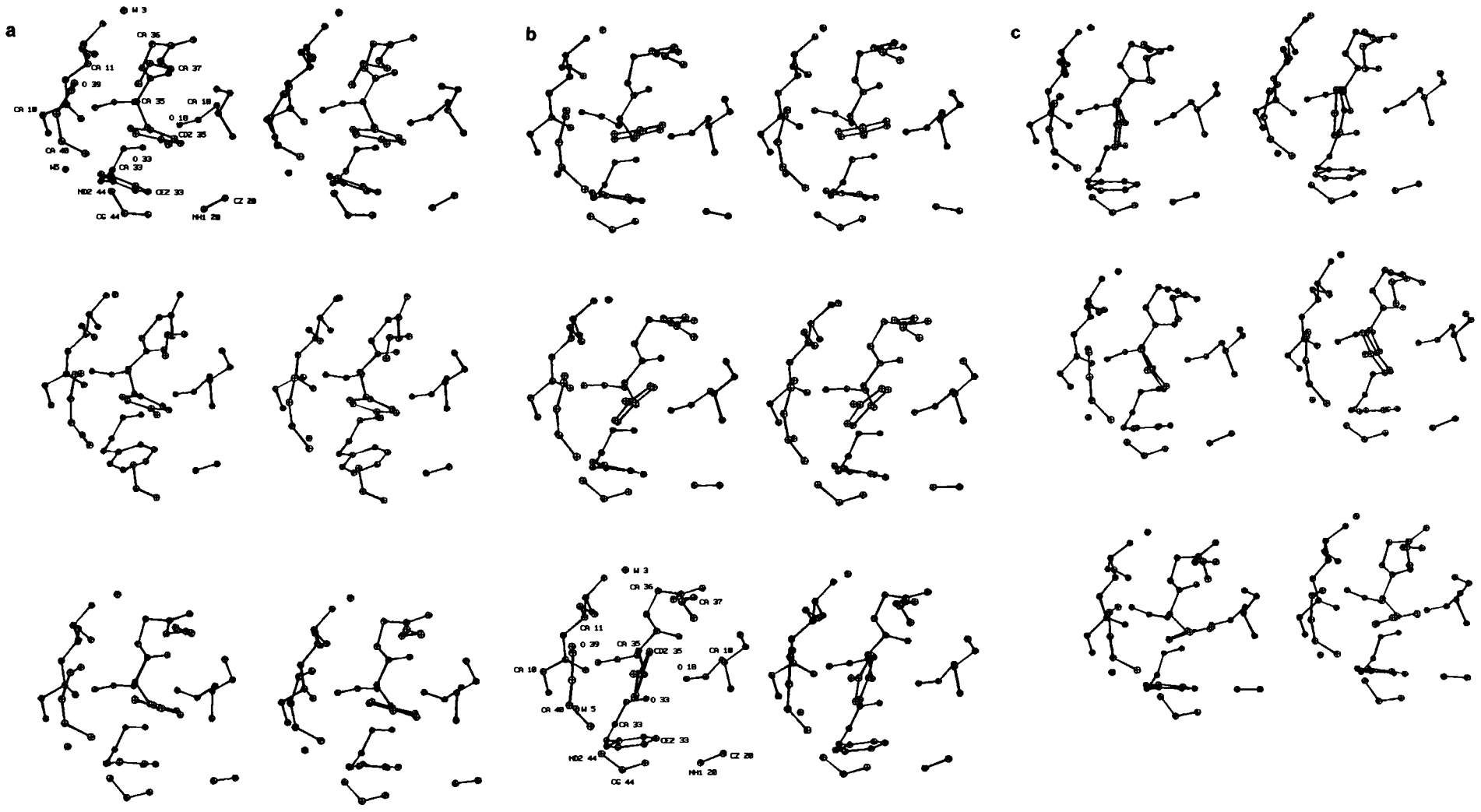

Figure 7. Configurations of atoms in the vicinity of tyrosine 35 at a sequence of times during the rotational isomerization. From top to bottom in each panel, the times in picoseconds are (a) 0.50, 0.75, 1.00, (b) 1.25, 1.38, 1.50, and (c) 1.62, 1.75, 2.00.

exhibit kinetics that are sensitive to the viscosity of the solvent. This behavior has been observed recently in ligand binding by heme proteins.[4,31] Formal methods for analyzing such gate/intrinsic decompositions are currently being developed (J. A. McCammon and S. H. Northrup); these methods are analogous to those presented recently for gated diffusion-influenced reactions.[32-34]

The important result that transient packing defects and gating play essential roles in local conformational changes within proteins illustrates that the protein matrix exhibits both liquid-like and solid-like characteristics.[2] The initial displacements of groups are facilitated by small packing defects similar to those that facilitate atomic diffusion in simple liquids.[14] Proteins differ from simple liquids, however, in that their extensive covalent and hydrogen bonding limits the compliance of the matrix to larger deformations. Thus, the matrix displays elastic behavior analogous to that of a solid in response to large displacements of groups.[2]

Finally, it should be noted that the methods employed in this study will be useful in the analysis of other group displacements in proteins. The construction of a suitable reaction coordinate is an essential first step in the theoretical calculation of rate constants, activation parameters, and other characteristics of reactions in proteins.[20] The present results make clear that it is necessary to include gating effects explicity in the construction of reaction coordinates for processes that involve substantial group displacements. In the ring rotational isomerization case, the virtual dihedral angle χ_v serves as a probe of the gate configuration. It is also clear that Voronoi polyhedra provide a valuable quantitative measure of the contribution of transient packing defects to group displacements in proteins.

Acknowledgment. We thank Drs. Bennett Fox and Witold Brostow for providing a copy of the Voronoi polyhedron program. This research was supported in part by grants from the Robert A. Welch Foundation and the NSF (Houston) and from the Petroleum Research Fund as administered by the American Chemical Society, and the Research Corp. (TN). C.Y.L. was a Welch Foundation Postdoctoral Fellow. J.A.M. is an Alfred P. Sloan Fellow and recipient of an NIH Research Career Development Award.

Registry No. BPTI, 9087-70-1; L-tyrosine, 60-18-4.

(31) Beece, D.; Eisenstein, L.; Frauenfelder, H.; Good, D.; Marden, M. C.; Reinisch, L.; Reynolds, A. H.; Sorensen, L. B.; Yue, K. T. *Biochemistry* **1980**, *19*, 5147.
(32) McCammon, J. A.; Northrup, S. H. *Nature (London)* **1981**, *293*, 316.
(33) Northrup, S. H.; Zarrin, F.; McCammon, J. A. *J. Phys. Chem.* **1982**, *86*, 2314.
(34) Szabo, A.; Shoup, D.; Northrup, S. H.; McCammon, J. A. *J. Chem. Phys.* **1982**, *77*, 4484.

Conformational Analysis of Proline Rings from Proton Spin–Spin Coupling Constants and Force-Field Calculations: Application to Three Cyclic Tripeptides[1a,b]

Frank A. A. M. de Leeuw,[1c] Cornelis Altona,*[1c] Horst Kessler,[1d] Wolfgang Bermel,[1d] Axel Friedrich,[1d] Gerhard Krack,[1d] and William E. Hull[1e]

Contribution from the Gorlaeus Laboratories, University of Leiden, 2300 RA Leiden, The Netherlands, Institut für Organische Chemie der Universität Frankfurt, Niederurseler Hang, D-6000 Frankfurt-50, Federal Republic of Germany, and Bruker Analytische Messtechnik GmbH, Silberstreifen, D-7512, Rheinstetten-Fo, Federal Republic of Germany (FRG). *Received July 21, 1982*

Abstract: The conformational analysis of the proline rings in the cyclic tripeptides *cyclo*(L-Pro$_3$), *cyclo*(L-Pro$_2$-D-Pro), and *cyclo*(L-Pro-BzlGly-D-Pro) is carried out by means of the vicinal proton spin–spin coupling constants. The combined use of a generalized Karplus equation and the concept of pseudorotation afforded a detailed description of the conformational behavior of each Pro ring in solution. The results correlate well with the spin–lattice ^{13}C relaxation time data obtained previously and with force-field calculations carried out on the three molecules. Experimental differences between pairs of cis couplings are explained in terms of contributions of alternative coupling pathways. Comparison with the geometries obtained by means of crystallographic analysis shows that in each case the conformation of the prolyl residues in the tripeptides found in the solid state also predominates in solution: in *cyclo*(L-Pro$_3$) between ${}^{\beta}_{\alpha}T$(C$^{\beta}$exo-C$^{\alpha}$endo) and ${}^{\beta}$E; in *cyclo*(L-Pro^1-L-Pro^2-D-Pro^3), first residue ${}^{\gamma}E$, second residue ${}^{\gamma}_{\beta}T$, and D-Pro^3 ${}^{\beta}E$; in *cyclo*(L-Pro^1-BzlGly-D-Pro^3), first residue ${}^{\gamma}_{\beta}T$, third residue ${}^{\beta}E$ (T and E are the twist and evelope conformation in the usual convention). According to the ^1H NMR analysis and force-field calculation *cyclo*(L-Pro$_3$) appears to adopt a conformationally pure crown conformation in solution. The three Pro residues oscillate over an unusually large range within a (quasi) double-minimum energy well. The backbone of *cyclo*(L-Pro^1-L-Pro^2-D-Pro^3) adopts a twist-boat conformation, which allows L-Pro^1 and L-Pro^2 sufficient conformational freedom to flip over into a (minor) ${}_{\gamma}E$ form. D-Pro^3 again oscillates over a large range. The situation is more complicated in the case of the third cyclic tripeptide *cyclo*(L-Pro^1-BzlGly-D-Pro^3). Force-field calculations suggest the existence of two twist-boat conformers, *TB*-1 and *TB*-2, which interconvert via a boat form with $\phi_2 \sim 0°$. Since it is also predicted that the Pro residues in each of these *TB*'s enjoy some conformational freedom, a multistate mixture is envisaged.

The conformational analysis of the proline ring is discussed in a large number of papers; cf. ref 2–7. In contrast to the fairly rigid chair form of six-membered rings, five-membered rings in general demonstrate pseudorotational mobility. The conforma-

(1) (a) Peptide Conformations. 20. Previous paper in this series: Kessler, H. *Angew. Chem.* **1982**, *94*, 509–520. (b) Related previous paper: Kessler, H.; Bermel, W.; Friedrich, A.; Krack, G.; Hull, W. E. *J. Am. Chem. Soc.* **1982**, *104*, 6297–6304. (c) University of Leiden. (d) University of Frankfurt. (e) Bruker Analytische Messtechnik.

(2) Kessler, H.; Friedrich, A.; Hull, W. E. *J. Org. Chem.* **1981**, *46*, 3892–3895.
(3) (a) Deber, C. M.; Torchia, D. A.; Blout, E. R. *J. Am. Chem. Soc.* **1971**, *93*, 4893–4897. (b) Anteunis, M. J.; Callens, R.; Asher, V.; Sleeckx, J. *Bull. Soc. Chim. Belg.* **1978**, *87*, 41–60.

0002-7863/83/1505-2237$01.50/0